WALAILAK JOURNAL
http://wjst.wu.ac.th MiniReview

Effective Efficiency of Solar Air Heaters of Different Types of Roughness Geometries over Absorber Plate

Maneesh KAUSHAL[1,*] and Varun GOEL[2]

[1]*Larsen and Toubro Limited, Engineering Design and Research Centre, Chennai 600089, India*
[2]*Department of Mechanical Engineering, National Institute of Technology, Hamirpur 177005, India*

([*]Corresponding author's e-mail: maneesh.nith@gmail.com)

Received: 29 April 2013, Revised: 25 November 2013, Accepted: 13 December 2013

Abstract

Artificial roughness has been found to enhance the rate of heat transfer in solar air heater ducts. However, improvement in heat transfer enhancement is invariably accompanied by increased pumping power. Several investigators have investigated the effect of different types of roughness on solar air heaters on the basis of heat transfer and friction factor. This paper presents a comparison of effective efficiency of solar air heaters of various types of roughness geometries over the absorber plate. These geometries have been used by various investigators in order to increase the heat transfer and friction factor in solar air heaters. Based upon correlations developed by various investigators, effective efficiency is also compared for a set of roughness geometries within the investigated range of operating parameters.

Keywords: Solar air heater, artificial roughness, heat transfer, thermohydraulic performance, friction factor

Introduction

Solar air heaters, because of their simplicity, are cheap and are the most widely used collection devices of solar energy [1]. The thermal performance of conventional solar air heaters has been found to be poor because of the low convective heat transfer coefficient from the absorber plate to the air flowing in the duct. The low value of the convective heat transfer coefficient is generally attributed to the presence of a laminar sub-layer on the heat transferring surface. Artificial rib roughness on the underside of the absorber plates has been found to be an efficient method for enhancing the performance of solar air heaters [2]. These ribs break the laminar boundary layer and make the flow turbulent adjacent to the wall, and this results in an increase in heat transfer. This also results in an increase in pressure drop due to increased friction. However, due to the increase in friction factor, the power consumed to propel or suck air by blowers through solar air heaters also increases substantially. It is therefore essential that the flow duct and artificial roughness employed to obtain the enhancement should be such that the maximum possible gain in heat transfer is achieved with the minimum possible friction loses [3-5]. Contrary to this, the excessive disturbance in the boundary layer creates more disturbance, and this results in more pumping power. Hence, turbulence must be created in the region of the laminar sub-layer only.

Zhang *et al*. [6] and Han *et al*. [7] studied the effect of artificial roughness on heat transfer and friction factor for 2 opposite roughened surfaces. However, in the case of solar air heaters, the roughness element has to be considered only on the underside of the one wall of duct which receives solar radiation. Therefore, solar air heaters are designed as rectangular channels, having one rough wall and three smooth walls. Based on the literature review, it is found that most of the investigations have been concentrated on the flow Reynolds number in solar air heaters of ranges of 2000 < Re < 16000.

Literature review for artificial roughness

Nikuradse [8] studied the effect of artificial roughness on the friction factor and the velocity distribution in pipes roughened by sand blasting. Nunner [9] and Dippery and Sebersky [10] developed a friction similarity law and a heat momentum transfer analogy for flow in sand grain roughened tubes. In solar air heaters, mostly rib type artificial roughness has been investigated. The ribs can be full (continuous) or discrete (broken) depending on whether the rib placed on the absorbing surface is complete or in pieces. The orientation of the ribs can be transverse, inclined, V-shaped, W-shaped, discrete V-shaped, discrete W-shaped, or multiple V-shaped. Han and Zhang [11] found that ribs inclined at an angle of attack of 45° resulted in better heat transfer performance when compared to transverse ribs. Lau *et al*. [12], Taslim *et al*. [13] and Hans *et al*. [17] investigated the effect of V-shaped ribs, and found that V-shaped ribs result in better enhancement in heat transfer in comparison to inclined ribs and transverse ribs. Ichimiya *et al*. [14] experimentally investigated the effect of porous type artificial roughness on the heat transfer and friction characteristics in a parallel plate rectangular duct. The rib roughness can also be identified in accordance with the cross section of ribs, such as square, rectangular, triangular, circular, semicircular, and trapezoidal ribs. Ravigururanjan and Bergles [15] used 4 types of roughness, namely semicircular, circular, rectangular, and triangular ribs, to develop the general statistical correlations for heat transfer and pressure drop in a single phase turbulent flow having internally ribbed surface. Liou and Hwang [16] tested 3 shapes of rib roughness, namely square, triangular, and semicircular ribs, to study the effect of rib shapes on turbulent heat transfer and friction in a rectangular channel with 2 opposite ribbed walls.

Study of roughness parameters and their effect on heat transfer and friction factor

Many investigators have investigated the effect of heat transfer and friction factor for roughened rectangular duct of solar air heaters. Hans *et al*. [17] investigated the effect of multiple v-ribs over the absorber plate, and found that maximum heat transfer and friction factor occurs at 60°. Yadav *et al*. [18] investigated the effect of heat transfer and friction characteristics of circular protrusions as artificial roughness. Lanjewar *et al*. [19] studied the effect of heat transfer and friction factor characteristics on a rectangular duct roughened with W-shaped ribs on the underside of the absorber plate. Momin *et al*. [20] investigated the effect of geometrical parameters of V-shaped rib roughness. The maximum enhancement of the Nusselt number was 2.3 times and of the friction characteristic was 2.83 times as compared to smooth duct. Sethi *et al*. [21] investigated the effect on heat transfer and friction factor in a roughened duct having dimple-shaped roughness geometry. The investigation covered a Reynolds number range of 2000 - 30000, a relative roughness height (e/D) of 0.02 - 0.045, and an angle of attack of flow (α) of 30° - 90° for a fixed relative pitch of 10. The correlations for heat transfer and friction factor developed by these investigators for different geometries of roughness element are given in **Table 1**.

Thermohydraulic performance (effective efficiency) of solar air heater

It is well known that the use of artificial roughness on the absorber plate of a solar air heater enhances its thermal efficiency as flow rate increases. However, a higher mass flow rate also results in higher friction losses. Also, the thermal performance of solar air heaters increases up to a certain limit of Reynolds number and then starts decreasing; this is accompanied by a certain pumping power penalty. The roughness geometry should be selected based on maximum thermal gain and minimum friction losses. Hence, the selection of roughness geometry has to be based on parameters that take thermohydraulic performance into account. Cortes and Piacentini [22] proposed effective efficiency for the purpose of such a comparison. Therefore, the pumping power required is converted to equipment thermal energy, in order to evaluate the real performance of the collector, in terms of the effective efficiency for the useful thermal gain, and the equivalent thermal energy that will be required to provide corresponding mechanical energy for overcoming friction power losses, This is given by;

$$\eta_{eff} = \frac{Q_u - \left(\frac{P_m}{C}\right)}{IA_p} \tag{1}$$

where $C = \eta_F \eta_M \eta_{Tr} \eta_{Th}$ is the conversion factor accounting for net conversion efficiency from the thermal energy of the resource to mechanical energy. The value of C is taken as 0.2 by taking the typical values in the conversion factor [C = Efficiency of fan or blower (0.75) × Efficiency of the electrical motor used for driving fan (0.9) × Efficiency of electrical transmission (0.9) × Thermal conversion efficiency of power plant (0.34)]

The effective efficiency has been computed for a set of geometries investigated by different investigators [17-21]. The typical values and other parameters used for current investigation are given in **Table 2**. The rate of useful energy gain and mechanical power consumed is given by the following expressions. Useful thermal energy gain;

$$Q_u = F'\left[I(\tau\alpha) - U_L(t_o - t_i)/2\right]A_p \tag{2}$$

where

$$F' = \frac{h}{h + U_L} \tag{3}$$

The useful thermal energy gain may also be calculated as;

$$Q_u = hA_p\left(t_p - t_f\right) \tag{4}$$

or

$$Q_u = mC_p\left(t_o - t_i\right) \tag{5}$$

Mechanical power consumed;

$$P_m = VA\ \Delta P \tag{6}$$

where

$$\Delta P = \left(2fLV^2\rho\right)/D \tag{7}$$

Hence

$$P_m = \rho fLV^3\left(W + H\right) \tag{8}$$

Table 1 Heat transfer coefficient and friction factor correlation for different roughness geometries.

Authors	Roughness geometry	Range of parameters	Correlations	
			Heat transfer coefficient	Friction factor
Hans *et al.* [17]	Multiple V-ribs	Re = 2000-20000 e/D_h = 0.019-0.043 p/e = 6-12 W/w = 1-10 α = 30°-75°	$h = 3.5\times10^{-5}\times \mathrm{Re}^{0.92}\times\left(\frac{e}{D_h}\right)^{0.77}\times\left(\frac{W}{w}\right)^{0.43}\times\left(\frac{\alpha}{90}\right)^{-0.49}\times\exp\left[-0.1177\left\{\ln\left(\frac{W}{w}\right)\right\}^2\right]\times\exp\left[-0.61\left\{\ln\left(\frac{\alpha}{90}\right)\right\}^2\right]\times\left(\frac{p}{e}\right)^{8.54}\times\exp\left[-2.0407\left\{\ln\left(\frac{p}{e}\right)\right\}^2\right]$	$f = 4.47\times10^{-4}\times \mathrm{Re}^{-0.3188}\times\left(\frac{e}{D_h}\right)^{0.78}\times\left(\frac{W}{w}\right)^{0.22}\times\left(\frac{\alpha}{90}\right)^{-0.39}\times\exp\left[-0.52\left\{\ln\left(\frac{\alpha}{90}\right)\right\}^2\right]\times\left(\frac{p}{e}\right)^{8.9}\times\exp\left[-2.133\left\{\ln\left(\frac{p}{e}\right)\right\}^2\right]$
Yadav *et al.* [18]	Circular protrusions	Re = 3600-18100 e/D_h=0.015-0.03 p/e = 12-24 α = 45°- 75°	$h = 0.154\times \mathrm{Re}^{1.017}\times\left(\frac{e}{D_h}\right)^{0.521}\times\left(\frac{p}{e}\right)^{-0.38}\times\left(\frac{\alpha}{60}\right)^{-0.213}\times\exp\left[-2.023\left\{\ln\left(\frac{\alpha}{60}\right)\right\}^2\right]$	$f = 7.207\times \mathrm{Re}^{-0.56}\times\left(\frac{e}{D_h}\right)^{0.176}\times\left(\frac{p}{e}\right)^{-0.18}\times\left(\frac{\alpha}{60}\right)^{0.038}\times\exp\left[-1.412\left\{\ln\left(\frac{\alpha}{60}\right)\right\}^2\right]$
Lanjewar *et al.* [19]	W-shaped roughness	Re = 2300-14000 p/e = 10 e/D_h = 0.018-0.3375 α = 30°-75° W/H = 8	$h = 0.0613\times \mathrm{Re}^{0.9079}\times\left(\frac{e}{D_h}\right)^{0.4487}\times\left(\frac{\alpha}{60}\right)^{-0.1331}\times\exp\left[-0.5307\left\{\ln\left(\frac{\alpha}{60}\right)\right\}^2\right]$	$f = 0.6182\times \mathrm{Re}^{-0.2254}\times\left(\frac{e}{D_h}\right)^{0.4622}\times\left(\frac{\alpha}{60}\right)^{-0.0817}\times\exp\left[-0.28\left\{\ln\left(\frac{\alpha}{60}\right)\right\}^2\right]$
Momin *et al.* [20]	V-shaped continuous ribs	Re = 2500-18000 e/D_h = 0.02-0.034 p/e = 10 α = 30°-90°	$h = 0.067\times \mathrm{Re}^{0.888}\times\left(\frac{e}{D_h}\right)^{0.424}\times\left(\frac{\alpha}{60}\right)^{0.077}\times\exp\left[-0.782\left\{\ln\left(\frac{\alpha}{60}\right)\right\}^2\right]$	$f = 6.266\times \mathrm{Re}^{0.425}\times\left(\frac{e}{D_h}\right)^{0.565}\times\left(\frac{\alpha}{60}\right)^{-0.093}\times\exp\left[-0.719\left\{\ln\left(\frac{\alpha}{60}\right)\right\}^2\right]$
Sethi *et al.* [21]	Dimple shape	Re = 3600-18000 e/D_h = 0.021-0.036 p/e = 10-20 α = 45°- 75°	$h = 7.1\times10^{-3}\times \mathrm{Re}^{1.1386}\times\left(\frac{e}{D_h}\right)^{0.3629}\times\left(\frac{p}{e}\right)^{-0.047}\times\left(\frac{\alpha}{60}\right)^{-0.0048}\times\exp\left[-0.7792\left\{\ln\left(\frac{\alpha}{60}\right)\right\}^2\right]$	$f = 4.869\times10^{-1}\times \mathrm{Re}^{-0.223}\times\left(\frac{e}{D_h}\right)^{0.3629}\times\left(\frac{p}{e}\right)^{-0.059}\times\left(\frac{\alpha}{60}\right)^{0.0042}\times\exp\left[-0.4801\left\{\ln\left(\frac{\alpha}{60}\right)\right\}^2\right]$

The equation for the effective efficiency of a solar air heater can be obtained by substituting the values of Eq. (2) and Eq. (8) in Eq. (1) as;

$$\eta_{eff} = \frac{(F'[I(\tau\alpha) - U_L(t_o - t_i)/2]A_p) - \left(\frac{\rho f L V^3 (W+H)}{C}\right)}{IA_p} \tag{9}$$

The term (τα) represents the product of transmittance and absorptance because it accounts for the complex interaction of optical properties of glass cover and absorber plate, (t_o-t_i) is the rise in temperature of fluid and F' is the collector efficiency factor. Eq. (9) can also be used to determine the effective efficiency of a smooth absorber plate solar air heater.

The value of pressure drop (ΔP) across the collector having flow velocity (V), length (L) and hydraulic diameter (D) is calculated by using the friction factor (f) from Eq. (7). The value of the coefficient of the heat transfer (h) and the friction factor (f) for a roughened absorber plate solar air heater have been determined from the correlation developed by investigators as given in **Table 1**, and for a smooth absorber plate solar air heater these values obtained from Dittus-Boelter and Blasius equation are;

$$h_s = 0.023 \text{ Re}^{0.8} \text{ Pr}^{0.4}\left(\frac{k}{D}\right) \tag{10}$$

$$f_s = 0.079 \text{ Re}^{-0.25} \tag{11}$$

Table 2 Typical values of operating and system parameters.

Parameters	**Value**
System parameters	
Collector length, L	1 (m)
Duct width, W	0.2 (m)
Duct height, H	0.02 (m)
Overall loss coefficient, U_L	10 (W/m^{2}K)
Thermal conductivity of insulation, k	0.0262 (W/mK)
Transmittance-absorptance product, τα	0.85
Relative roughness height, e/D_h	0.02 - 0.045
Relative roughness pitch, P/e	10
Reynolds number, Re	2000 - 30000
Angle of attack, α	30° - 90°
Operating parameters	
Ambient temperature, T_a	300 (K)
Specific heat, C_p	1005.6 (J/kgK)
Solar insulation, I	800 (W/m^2)

Results and discussion

As mentioned above, the thermo-hydraulic performance (effective efficiency) of roughened as well as smooth absorber plates of solar air heaters has been calculated on the basis of the method proposed by Cortes and Piacentini [22]. Relative roughness height (e/D_h) is considered to be the strongest parameter for the effective efficiency calculation of solar air heaters. The effective efficiencies of solar air heaters or collectors have been plotted as a function of Reynolds number in **Figures 1 - 5**, which shows that effective efficiency attains a maximum value at a certain Reynolds number and thereafter starts decreasing. This may be due to the dominance of pumping (mechanical) power which is required to overcome the frictional forces in the solar air heater duct. From **Figures 1 - 5** it can be observed that, for a given value of roughness parameters, a similar trend in variation of effective efficiency is obtained with the Reynolds number. It shows that there exists an optimum operating roughness parameter for which effective efficiency is at maximum. It is also observed that, for higher values of relative roughness height (e/D_h), effective efficiency is better with a lower range of Reynolds number; however, the value of effective efficiency is reversed in a higher range of Reynolds number.

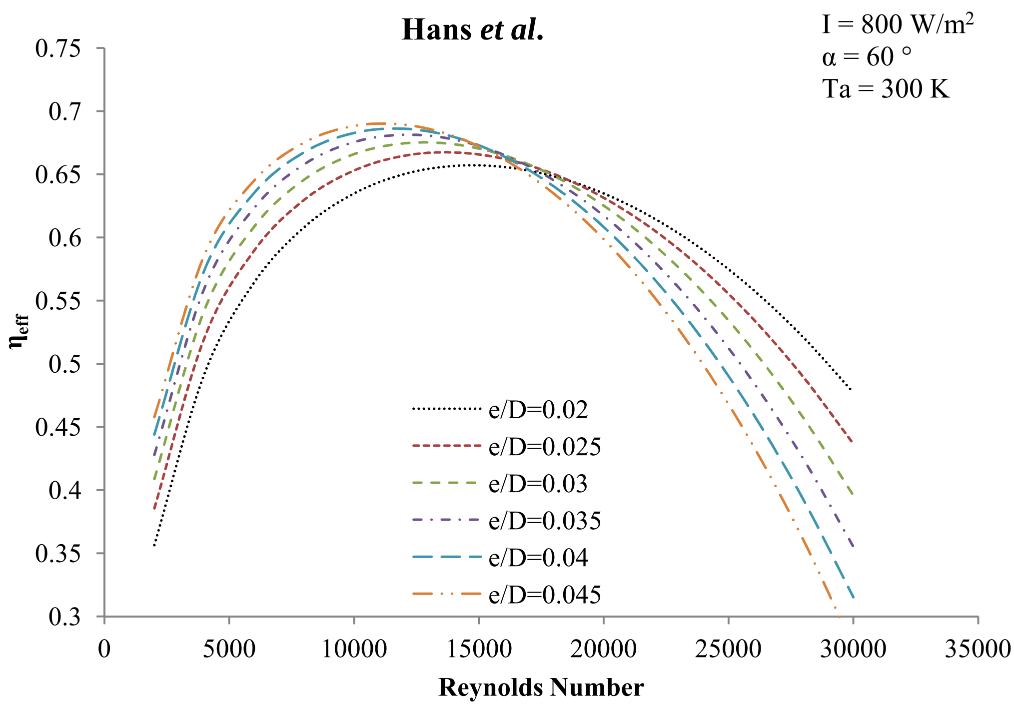

Figure 1 Effective efficiency vs Reynolds number for the roughness geometry used by Hans *et al*. for 6 values of e/D_h.

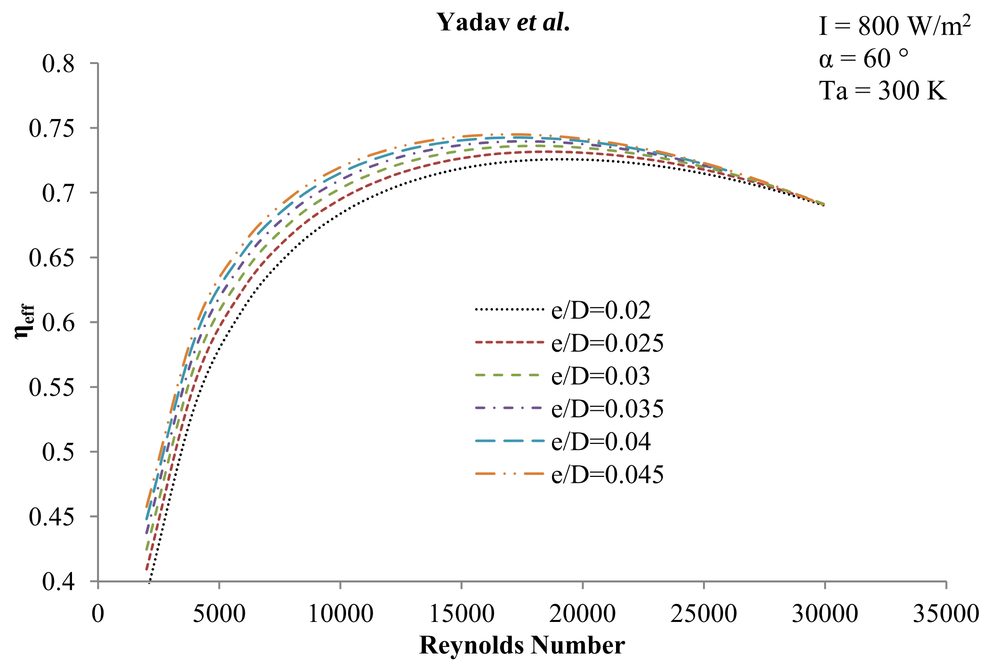

Figure 2 Effective efficiency vs Reynolds number for the roughness geometry used by Yadav *et al*. for 6 values of e/D_h.

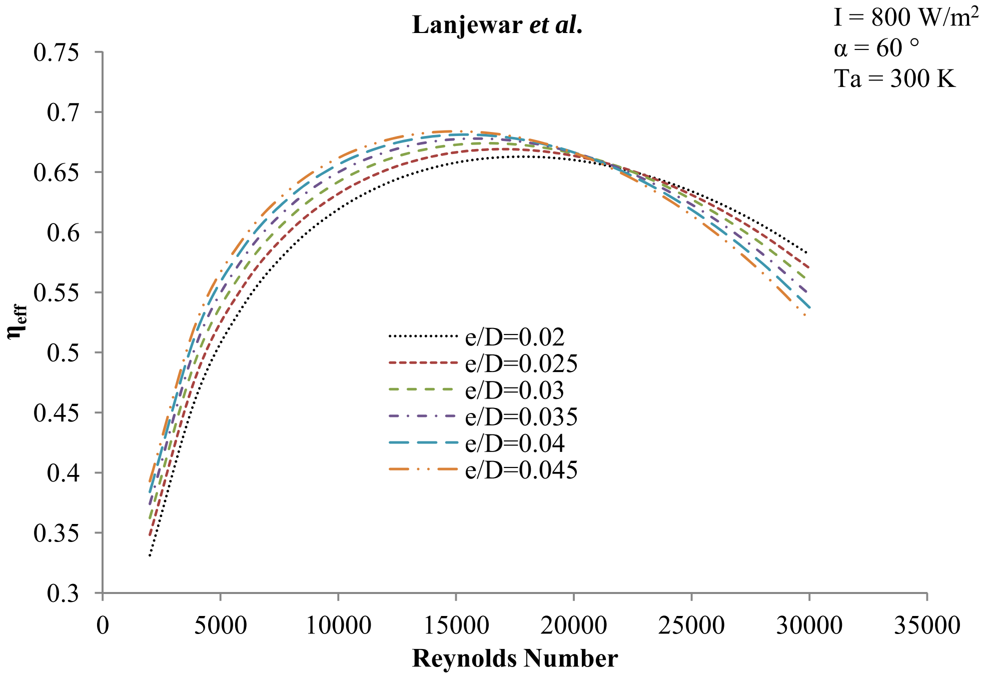

Figure 3 Effective efficiency vs Reynolds number for the roughness geometry used by Lanjewar *et al*. for 6 values of e/D_h.

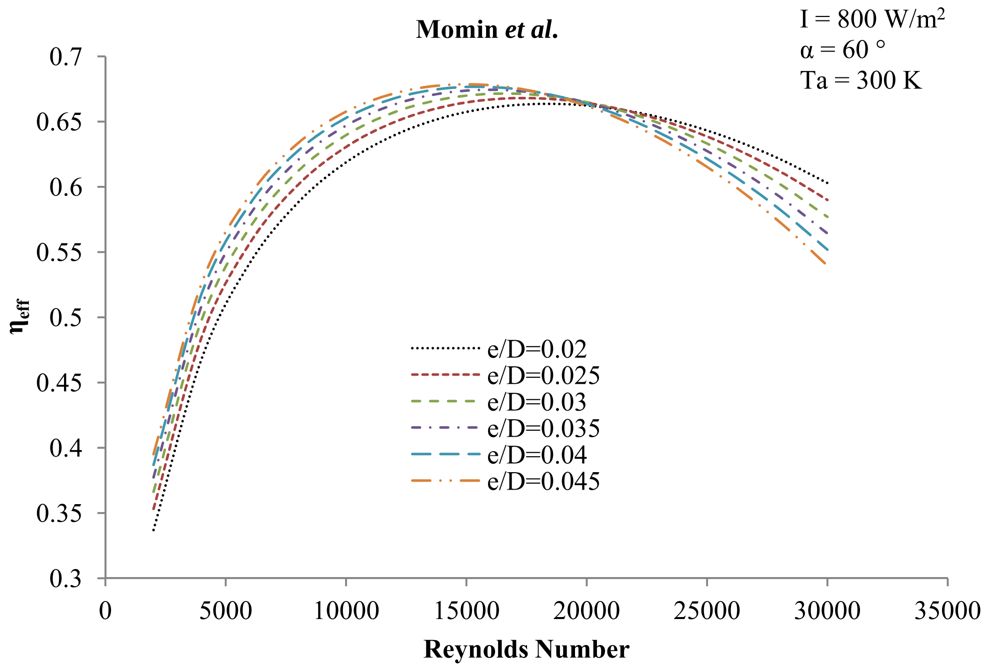

Figure 4 Effective efficiency vs Reynolds number for the roughness geometry used by Momin *et al*. for 6 values of e/D_h.

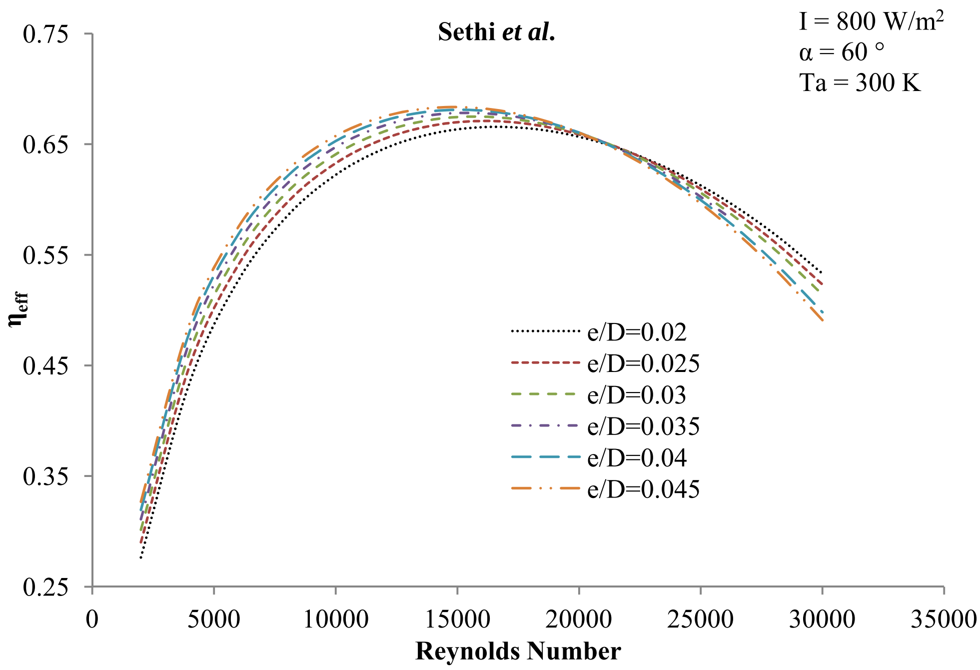

Figure 5 Effective efficiency vs Reynolds number for the roughness geometry used by Sethi *et al*. for 6 values of e/D_h.

The effect of relative roughness height on effective efficiency is insignificant at a lower Reynolds number as compared to that at a higher Reynolds number. At a higher range of Reynolds numbers, the effective efficiency increases, with a decrease in relative roughness height for a given Reynolds number. It is observed that the Reynolds number at which the effective efficiency attains a maximum value depends on the relative roughness height (e/D_h). **Figure 6** has been prepared to compare the effective efficiencies of solar air heaters having different roughness geometries. It is observed that among all of the roughness geometries, the circular protrusions arrangement has maximum effective efficiency in a higher range of Reynolds number (more than 14000). However, multiple v-ribs have a maximum effective efficiency in a lower range of Reynolds number (less than 12000). Further, it is also observed that the effective efficiency of smooth solar air heaters is better than the roughened solar air heaters in a higher range of Reynolds number.

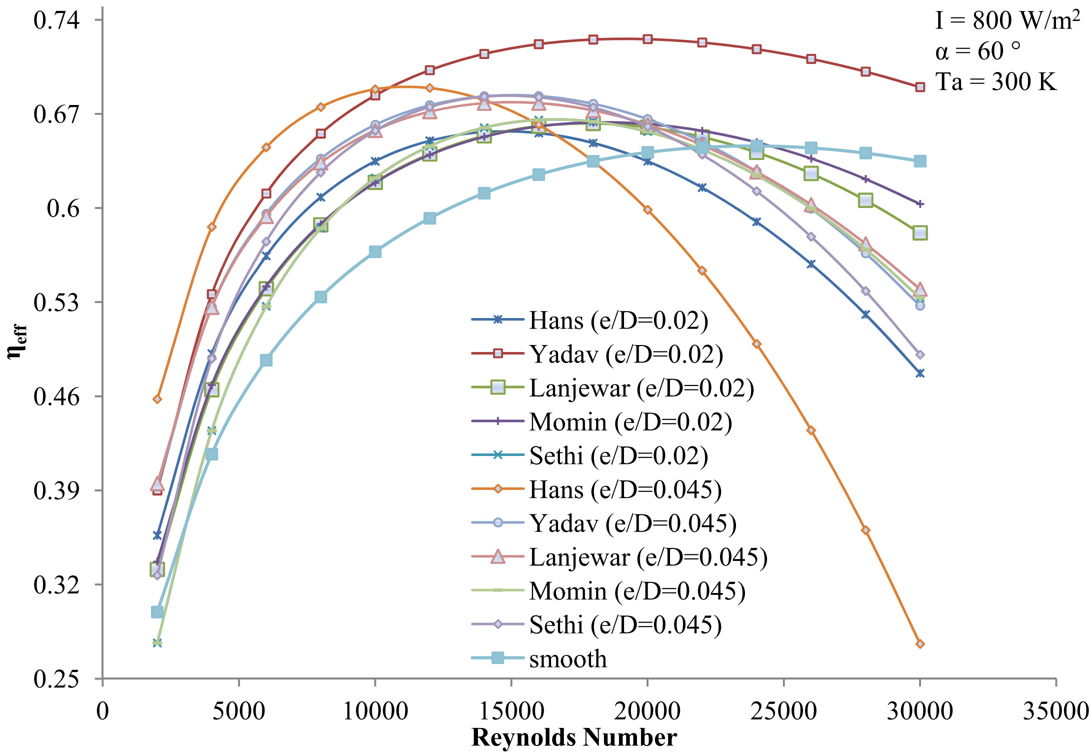

Figure 6 Comparison of effective efficiency vs Reynolds number for roughened and smooth air heaters.

Conclusions

Effective efficiency was calculated at different angles of attack and at different relative roughness height. It was found that effective efficiency is higher at a 60 ° angle of attack. There was a considerable enhancement in the effective efficiency of solar air heaters having a roughened duct provided with different types of roughness elements. Solar air heaters having circular protrusions as roughness elements were found to have better effective efficiency in a higher range of Reynolds number. However, multiple v-ribs geometry was found to be suitable in the lower range of Reynolds number.

References

[1] MK Mittal, Varun, RP Saini and SK Singal. Effective efficiency of solar air heaters having different types of roughness elements on the absorber plate. *Energy* 2007; **32**, 739-45.
[2] Varun, RP Saini and SK Singal. A review on roughness geometry used in solar air heaters. *Sol. Energ.* 2007; **81**, 1340-50.
[3] K Prasad and SC Mullick. Heat transfer characteristics of solar air heater for drying purposes. *Appl. Energ.* 1985; **12**, 83-93.
[4] B Prasad and JS Saini. Effect of artificial roughness on heat transfer on heat transfer and friction factor in solar air heater. *Sol. Energ.* 1985; **41**, 555-60.
[5] JL Bhagoria, JS Saini and SC Solanki. Heat transfer coefficient and friction factor correlation for rectangular solar air heater duct having transverse wedge shape rib roughness on the absorber plate. *Renew. Energ.* 2002; **25**, 341-69.
[6] YM Zhang, WZ Gu and HQ Xu. Enhancement of heat transfer and flow characteristics in rib roughened rectangular channels. *J. Eng. Thermophys.* 1984; **5**, 275-80.
[7] JC Han, LR Glicksman and WM Rohsenow. An investigation of heat transfer and friction for rib roughened surfaces. *Int. J. Heat Mass Tran.* 1978; **21**, 1143-56.
[8] J Nikuradse. *Laws of Flow in Rough Pipes*. NACA, Technical Memorandum 1292, 1950.
[9] W Nunner. *Heat Transfer and Pressure Drop in Rough Tubes*. AERE Lib Transactions, 1958.
[10] DF Dippery and RH Sabersky. Heat and momentum transfer in smooth and rough tubes at various Prandtl number. *Int. J. Heat Mass Tran.* 1963; **6**, 329-53.
[11] JC Han and YM Zhang. High performance heat transfer ducts with parallel, broken and V-shaped broken ribs. *Int. J. Heat Mass Tran.* 1992; **35**, 513-23.
[12] SC Lau, RT Kukraja and RD McMillin. Effect of V-shaped rib arrays on turbulent heat transfer and friction of fully developed flow in a square channel. *Int. J. Heat Mass Tran.* 1991; **34**, 1605-16.
[13] ME Taslim, T Li and DM Kercher. Experimental heat transfer and friction in channels roughened with angled, V-shaped and discrete ribs on two opposite walls. *ASME J. Turbomach.* 1996; **118**, 20-8.
[14] K Ichimiya, M Katayama, T Miyazawa and H Kondoh. Experimental study on effects of a single porous type roughness element in a parallel plate duct. *Exp. Heat Tran.*1991; **4**, 319-30.
[15] TS Ravigururajan and AE Bergles. General correlation for pressure drop and heat transfer for single-phase turbulent flow in internally ribbed tubes: augmentation of heat transfer in energy systems. *ASME HTD* 1985; **52**, 9-20.
[16] TM Liou and JJ Hwang. Developing heat transfer and friction in a rectangular ribbed duct with flow separation at inlet. *ASME J. Heat Tran.* 1992; **114**, 565-73.
[17] VS Hans, RP Saini and JS Saini. Heat transfer and friction factor correlations for a solar air heater duct roughened artificially with multiple V-ribs. *Sol. Energ.* 2010; **84**, 898-911.
[18] S Yadav, M Kaushal, Varun and Siddhartha. Nusselt number and friction factor correlations for solar air heater duct having protrusions as roughness elements on absorber plate. *Exp. Therm. Fluid Sci.* 2013; **44**, 34-41.
[19] A Lanjewar, JL Bhagoria and RM Sarviya. Heat transfer and friction in solar air heater duct with W-shaped rib roughness on absorber plate. *Energy* 2011; **36**, 4531-41.
[20] AME Momin, JS Saini and SC Solanki. Heat transfer and friction in solar air heater duct with V-shaped ribs roughness on absorber plate. *Int. J. Heat Mass Tran.* 2002; **45**, 3383-96.
[21] M Sethi, Varun and NS Thakur. Correlations for solar air heater duct with dimpled shape roughness elements on absorber plate. *Energy* 2012; **86**, 2852-61.
[22] A Cortes and R Piacentini. Improvement of the efficiency of a bare solar collector by means of turbulent promoters. *Appl. Energ.* 1990; **36**, 253-61.